JOURNAL OF VIROLOGY, Dec. 2007, p. 13149–13157 Vol. 81, No. 23
0022-538X/07/$08.00+0 doi:10.1128/JVI.01415-07

Affinity Thresholds for Membrane Fusion Triggering by Viral Glycoproteins▽

Kosei Hasegawa,[1] Chunling Hu,[1] Takafumi Nakamura,[1]† James D. Marks,[2] Stephen J. Russell,[1] and Kah-Whye Peng[1]*

Molecular Medicine Program, Mayo Clinic College of Medicine, Rochester, Minnesota 55905,[1] and Department of Anesthesia, University of California San Francisco, San Francisco, California 94110[2]

Received 28 June 2007/Accepted 29 August 2007

Enveloped viruses trigger membrane fusion to gain entry into cells. The receptor affinities of their attachment proteins vary greatly, from 10^{-4} M to 10^{-9} M, but the significance of this is unknown. Using six retargeted measles viruses that bind to Her-2/neu with a 5-log range in affinity, we show that receptor affinity has little impact on viral attachment but is nevertheless a key determinant of infectivity and intercellular fusion. For a given cell surface receptor density, there is an affinity threshold above which cell-cell fusion proceeds efficiently. Suprathreshold affinities do not further enhance the efficiency of membrane fusion.

Enveloped viruses gain entry into cells by membrane fusion. This is mediated by viral membrane glycoproteins whose affinities for their receptors vary widely from the millimolar range (e.g., for influenza virus) to the nanomolar range (e.g., for human immunodeficiency virus [HIV]) (18, 40, 43–45, 47). Because of their high mutation rates, viruses can easily modulate the receptor affinities of their attachment glycoproteins under selective pressure. Changing receptor specificity requires a more radical alteration to the sequence of the attachment glycoprotein. Currently, little is known about the evolutionary pressures that determine the receptor affinities of enveloped viruses. Higher affinities might lead to more efficient binding to receptor-positive cells, but the high avidity of viral attachment would be expected to negate this advantage at a higher receptor density (17). Alternatively, higher affinities might somehow accelerate the postbinding events that lead to membrane fusion, thereby enhancing the efficiencies of viral entry and intercellular fusion between infected and uninfected cells. Conversely, excessive viral affinities might lead to viral mislocalization, infection of nontarget cells, or failure of the progeny virions to escape from the cell in which they were made.

In this study, we tested the impact of receptor affinity on virus-mediated membrane fusion by generating a panel of measles viruses displaying HER2/neu-specific single-chain variable fragment (scFv) antibodies with scFv-HER2 affinities ranging from 1.6×10^{-6} M to 1.5×10^{-11} M, and we characterized them with a panel of cells expressing various numbers of HER2 receptors. Measles virus (MV) is a negative-strand RNA virus belonging to the family *Paramyxoviridae*. The virus was originally isolated in 1954 from the throat of a patient with measles (6) and has since been subjected to serial tissue culture passage to create an attenuated (Edmonston) vaccine strain (7) that is showing considerable promise in oncolytic virotherapy studies (4, 10, 30, 32, 33). Oncolytic measles viruses use either one of two receptors to infect their target cells: CD46, which is expressed on all human nucleated cells (5, 24), or the signaling lymphocyte activation molecule (SLAM), which is expressed on activated T cells, B cells, and monocytes (14, 46). The viral attachment protein (hemagglutinin [HA]) binds to one or the other of these receptors and then catalyzes the fusion of virus and cell membranes by inducing a conformational rearrangement in the fusion (F) protein, leading to viral entry (15). Newly synthesized measles HA and F proteins accumulate on the surface of infected cells and mediate their fusion with neighboring receptor-positive cells to form multinucleated nonviable syncytia which die by apoptosis (8).

We recently generated fully retargeted measles viruses that are unable to enter cells via the native receptors CD46 and SLAM but which propagate efficiently and exclusively via alternative cellular receptors (11, 23, 48). New tropisms are conferred by scFvs displayed on the viral surface as C-terminal extensions on the mutated HA protein and are stably maintained during multiple serial virus passages without reversion to native receptor usage (11). In contrast to the other viruses for which this has been attempted (21, 31, 50), MV has a remarkably flexible and adaptable entry mechanism that can utilize multiple alternative cellular receptors.

The HER2/neu receptor (ErbB-2) is a well-established, therapeutically validated cancer target (39, 42). HER2/neu is a 185-kDa type I transmembrane glycoprotein belonging to the epidermal growth factor tyrosine kinase receptor family and is encoded by the *erbB2* gene (29). HER2/neu is overexpressed on tumor cells of 25 to 30% of breast cancer and ovarian cancer patients (19, 41), but it is expressed at low levels or not at all in adult normal tissues (25, 34). An anti-HER2/neu antibody, trastuzumab (Herceptin), is approved by the U.S. Food and Drug Administration for the treatment of patients with metastatic breast cancer and is being tested in clinical trials with ovarian cancer patients (3, 35). There is much interest in HER2/neu as a cancer target, and a variety of targeted

* Corresponding author. Mailing address: Molecular Medicine Program, Mayo Clinic College of Medicine, 200 First Street SW, Rochester, MN 55905. Phone: (507) 284-8357. Fax: (507) 284-8388. E-mail: peng.kah@mayo.edu.

† Present address: Department of Molecular Genetics, Medical Institute of Bioregulation, Kyushu University, Fukuoka 812-8582, Japan.

▽ Published ahead of print on 5 September 2007.

TABLE 1. Dissociation constants for the panel of scFvs for HER2/neu antigen and the recombinant measles viruses displaying the respective scFv

scFv	K_d (M) of scFv	Recombinant measles viruses
C6.5Y100kA	1.6×10^{-6}	MV-αHER-6
C6.5G98A	3.2×10^{-7}	MV-αHER-7
C6.5	1.6×10^{-8}	MV-αHER-8
C6ML3–9	1.0×10^{-9}	MV-αHER-9
C6MH3B1	1.2×10^{-10}	MV-αHER-10
C6B1D2	1.5×10^{-11}	MV-αHER-11

therapeutics have been developed and tested (20). In particular, a panel of scFvs that recognize the corresponding epitope on the HER2/neu receptor but bind with different affinities has been generated and characterized (Table 1). The C6.5 anti-HER2 scFv has an affinity of 1.6×10^{-8} M for the extracellular domain of HER2/neu and was selected from a nonimmune human scFv phage library (37). Using site-directed mutagenesis of the variable light- and heavy-chain CDR3 regions, CDR3 C6.5 antibody affinity mutants with dissociation constants ranging from 1.6×10^{-6} M to 1.5×10^{-11} M were generated (38). These anti-HER2 scFvs have generally similar association rate constants (k_{on}) but differ predominantly in their dissociation rate constants (k_{off}).

Given the appeal of HER2 as a cancer target and the availability of a very-well-characterized family of phage-selected anti-HER2 scFv affinity mutants and the natural variability of HER2 receptor expression levels with human tumors, we decided to make a panel of HER2-retargeted measles viruses with different HER2 affinities and to explore the relationship between HER2 affinity and receptor density and the efficiencies of viral entry, cell fusion, and cell killing. Avidity is expected to be high since these viruses have a few hundred copies of the attachment protein on the virion surface. Thus, we were keen to determine whether the scFv affinity of each of these multivalent viruses might even influence the biology of these viruses. Interestingly, our data show that infection and cell-to-cell fusion require a threshold affinity. Above a certain threshold affinity, fusion proceeds efficiently, regardless of how far the threshold is exceeded. This threshold affinity also varies depending on the receptor density on the target cells.

MATERIALS AND METHODS

Cell culture. Cell lines were purchased from the American Type Culture Collection (Manassas, VA) or have been described previously (13, 22, 32). CHO-HER2 clones expressing different densities of HER2 were established by stable transfection of pcDNA3.1-HER2 (kindly provided by Ralf G. Janknecht, Mayo Clinic, Rochester, MN) into CHO cells, followed by G418 selection (1 mg/ml).

Generation of fully retargeted HER2 recombinant measles viruses displaying different affinity mutants. The cDNA for the C6.5Y100kA, C6.5G98A, C6.5, C6ML3-9, C6H3B1, and C6B1D2 anti-HER2 scFv affinity mutants (38) was PCR amplified as SfiI/NotI fragments and inserted in-frame into the pTNH6aa shuttle vector coding for alanine substitution at residues 481 and 533 of measles HA proteins (22). The PacI/SpeI-digested fragment of each pTNH6-HER2scFv was inserted into the corresponding site of p(+)MV-eGFP, respectively. For the rescue of each HER2-retargeted virus, we used the hexahistidine (His_6) tagging and retargeting system as described previously (22). Virus stocks were harvested after the infection of Vero-anti-His (αHis) cells at a multiplicity of infection (MOI) of 0.03, and cell-associated viruses were harvested by freeze-thaw cycles. Viral stocks were titrated by 50% tissue culture infective dose ($TCID_{50}$) assay with Vero-αHis cells.

Immunoblotting. Equivalent amounts of infectious viruses (10^4 $TCID_{50}$; with the viral titer determined with Vero-αHis cells) were mixed with an equal volume of sodium dodecyl sulfate (SDS) loading buffer (130 mM Tris [pH 6.8], 20% glycerol, 10% SDS, 0.02% bromophenol blue, 100 mM dithiothreitol). These samples were denatured for 5 min at 95°C, separated on a 10% SDS-polyacrylamide gel, blotted to polyvinylidene difluoride membrane (Amersham, Piscataway, NJ), and immunoblotted with antimeasles N and HA protein as described previously (22).

Virus titration and infection. To compare growth characteristics of the recombinant viruses, Vero-αHis cells were infected with the panel of viruses at an MOI of 3.0 for 3 h at 37°C. The inoculum was removed, the standard medium was replaced, and the cells were maintained at 32°C. At 24, 48, and 72 h after infection, cells were scraped into 1 ml of Opti-MEM medium (Gibco BRL, Rockville, MD), and cell-associated viruses were released by two freeze-thaw cycles. Viral titers were determined by $TCID_{50}$ titration with Vero-αHis cells. For viral infection, cells were incubated with virus at an MOI of 1.0 and 4.0 for 3 h at 37°C and growth medium (with or without fusion inhibitory peptide) was replaced (FIP; Bachem, Torrance, CA). At 48 or 72 h after infection, cells were photographed and analyzed.

Virus binding assay. The SKOV3ip.1 cells (4×10^4) in 24-well plates were washed with cold medium and prechilled by placing the plates on ice for at least 30 min. Cells were incubated with viruses (diluted in cold Opti-MEM medium) at an MOI of 0.5 on ice for 5, 10, 20, or 40 min. Cells were washed three times with cold medium to remove unbound virus and maintained at 37°C in the presence of FIP for 48 h. Numbers of green fluorescent protein (GFP)-positive cells were counted.

Quantification of cell surface HER2 molecules. Cells were incubated with phycoerythrin-conjugated anti-HER2 antibody (BD Biosciences Pharmingen, San Diego, CA) or with control isotype-matched antibody. The number of HER2 receptors per cell was estimated using a BD QuantiBrite phycoerythrin quantitation kit (Becton Dickinson, San Jose, CA) by flow cytometry, as described previously (28).

Quantitation of syncytium sizes. To evaluate the cytopathic effects induced by HER2-retargeted viruses, we quantitated the extent of cell-to-cell fusion by counting the number of nuclei in each syncytium and representing it as a "syncytial index." Cells (3×10^5) in six-well plates were infected by virus at low MOIs of 0.02 and 0.1. After 72 h, cells were fixed with 0.5% glutaraldehyde, stained with Hoechst 33342 (Molecular Probes, Eugene, OR), and evaluated with fluorescence microscopy. Syncytia ($n = 10$ to 20) were randomly chosen, and numbers of nuclei in each syncytium were counted.

Apoptosis assay. Apoptosis was evaluated by detection of cytoplasmic histone-associated DNA fragments. Cells (5×10^3) in 96-well plates were incubated with virus at an MOI of 1.0. Seventy-two hours after infection, the cells were evaluated for apoptosis by using a cell death detection ELISAPLUS kit (Roche Diagnostics, Indianapolis, IN) according to the manufacturer's protocol. The data are expressed as the increase (n-fold) in optical density (at 405 nm) compared with that of untreated control cells.

Clonogenic assay. Cells (5×10^4) in 24-well plates were exposed to virus at an MOI of 1.0 and incubated for 72 h at 37°C. Thereafter, the cells were trypsinized, serially diluted, replated in six-well plates, and incubated undisturbed for 8 to 12 days to allow colony formation. Cells were then fixed with 2.5% glutaldehyde and stained with 2% crystal violet. Numbers of colonies in wells containing 100 to 200 colonies that were well separated from each other were counted for all viruses. The number of cells per colony was estimated by examining colonies with a light microscope. Only colonies estimated to have 50 or more cells were counted.

Statistical analysis. Statistical comparisons between the groups were made using one-way analysis of variance; if significant, comparisons were followed by Dunnett's multiple comparison test compared with the MV-αHER-8-treated group (displaying C6.5, parental αHER2 scFv). We used GraphPad Prism 3.0 (GraphPad software, San Diego, CA) for the statistical calculations. A P value of <0.05 was considered significant.

RESULTS

Generation and characterization of HER2-retargeted measles viruses. The family of anti-HER2 C6.5 scFv affinity mutants that we used in this study was previously generated by mutating the V_L and V_H CDR3 regions of C6.5 (37, 38). The cDNA of each scFv was PCR amplified as a SfiI/NotI fragment

and inserted into the shuttle vector pTNH6aa, thus placing the scFv as a C-terminal extension on measles HA protein (Fig. 1A). Alanine substitutions at residues 481 (Y→A) and 533 (R→A) of the measles HA protein, which, respectively, ablate CD46- and SLAM-mediated viral entry and cell fusion were introduced (Fig. 1A). The HA-scFv fragment was subcloned as a PacI/SpeI insert into the full-length infectious cDNA clone of the attenuated Edmonston MV strain expressing an enhanced GFP (eGFP) reporter gene, p(+)MV-eGFP (Fig. 1A). Since the viruses are doubly ablated for CD46 and SLAM interaction, a His_6 tag inserted at the C terminus of hemagglutinin allows rescue, propagation, and titration of all six of the HER2 fully retargeted measles viruses via binding of the His_6 peptide to its pseudoreceptor (anti-His_6 scFv) on Vero-αHis cells, as described previously (22) (Table 1).

To confirm that the chimeric anti-HER2 scFv displaying hemagglutinin proteins were efficiently incorporated into virions, the viruses were loaded onto a 7.5% SDS-polyacrylamide gel, and HA proteins were detected using a rabbit polyclonal antibody recognizing the HA cytoplasmic tail (Fig. 1B). All chimeric HA proteins had a higher apparent molecular weight than those of the parental MV-eGFP virus. To estimate the relative particle-to-infectivity ratios of the retargeted and the parental viruses, the membrane was stripped and reprobed for the major MV structural nucleocapsid (N) protein. Dosimetric measurement of band intensities on the immunoblot indicates that the N and HA protein contents do not differ significantly between the viruses (Fig. 1B). Since equivalent amounts of infectious virus ($TCID_{50}$ of 10^4) were loaded per lane, these data suggest approximately comparable particle-to-infectivity ratios within the panel of HER2-retargeted viruses and between the HER2 viruses and the parental MV-eGFP virus. To compare the replication kinetics of the HER2-retargeted measles viruses via the αHis pseudoreceptor, lysates of virus-infected (MOI of 3.0) Vero-αHis cells were harvested at 24, 48, and 72 h postinfection, and viral titers were determined with Vero-αHis cells. The one-step growth curves of all six viruses were comparable (data not shown).

To show that the displayed anti-HER2 scFvs could mediate HER2 receptor-specific MV entry and syncytium formation, we used a panel of CHO cell transfectants expressing CD46, SLAM, HER2, or αHis (Fig. 1C). Each of these cell lines was infected with each of the HER2 scFv-displaying measles viruses (MV-αHER-6, -7, -8, -9, -10, and -11) and with the nontargeted MV-eGFP virus or a control CD38-retargeted MV-CD38 virus. The infected monolayers were photographed after 48 h. These data confirmed that all of the retargeted viruses lost their tropisms for CD46 and SLAM but gained the ability to enter cells via HER2 and via the αHis pseudoreceptor. As shown in Fig. 1C, it is apparent that the HER2-retargeted viruses displaying lower-affinity antibodies have a reduced ability to mediate membrane fusion via the HER2 receptor.

Receptor affinity and viral infection. To test the impact of receptor affinity on MV attachment, we mixed each of the viruses with prechilled medium and incubated them with HER2-positive human ovarian SKOV3ip.1 cancer cells on ice. Unbound virions were removed by washing with cold phosphate-buffered saline, and cells were returned to incubate at 37°C for 48 h, after which the numbers of infected GFP-

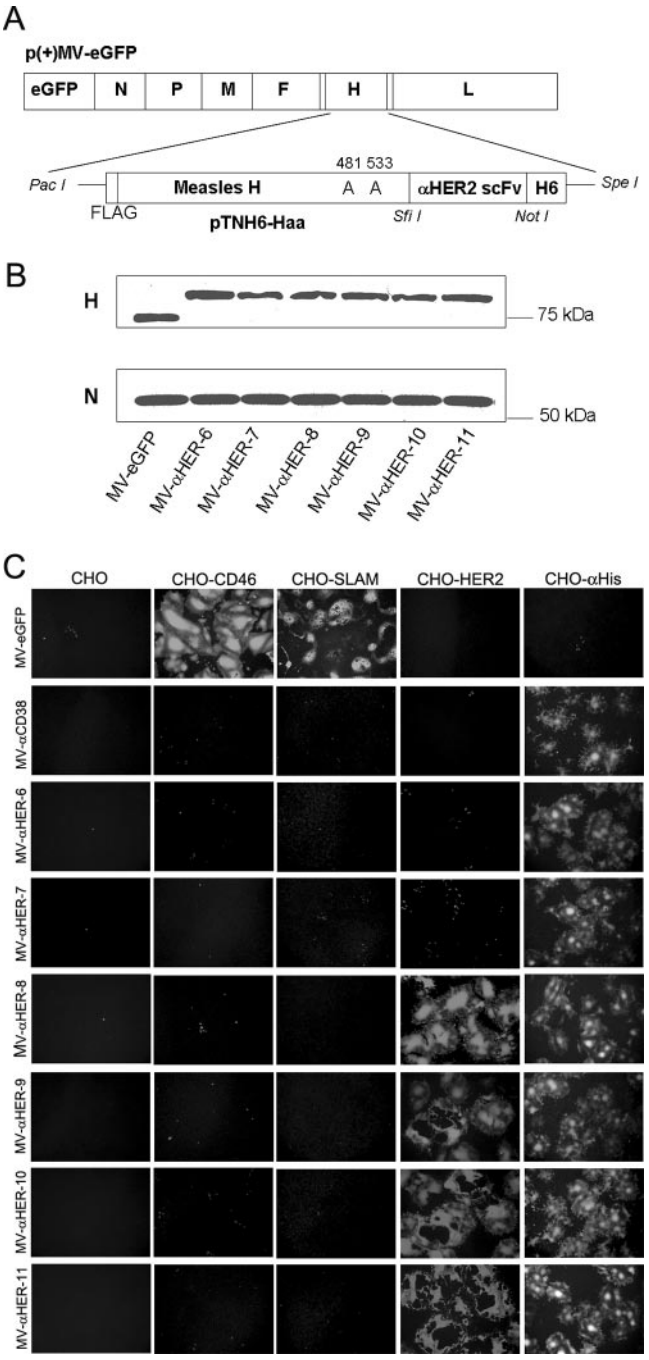

FIG. 1. Characterization of the HER2/neu-retargeted measles viruses. (A) Schematic representation of the HER2-retargeted viruses. The Y481A and R533A mutations ablate CD46 and SLAM interactions. The scFv was inserted as a SfiI/NotI fragment and displayed as a C-terminal extension on mutated HA proteins with a His_6 tag. (B) Immunoblotting results of the parental and HER2-retargeted virions using anti-HA and anti-N antibodies. Equal titers of each virus were loaded. (C) Specificity of the receptor usage of parental and fully retargeted anti-HER2 measles viruses. CHO cells and CHO cells stably expressing CD46, SLAM, HER2, or αHis were infected with the parental MV-eGFP, the CD38-retargeted, or the HER2-retargeted measles viruses at an MOI of 1.0. Cells were photographed with fluorescence microscopy after 48 h.

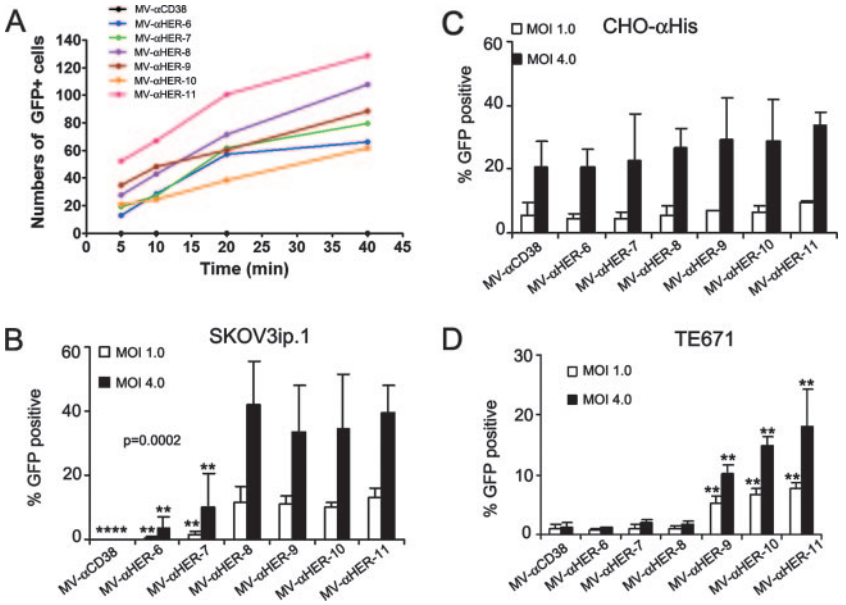

FIG. 2. The impact of receptor affinity on virus binding and infectivity. (A) There is no correlation between receptor affinity and virus binding with SKOV3ip.1 cells. HER2-retargeted viruses were allowed to bind to SKOV3ip.1 cells on ice for various times, after which unbound viruses were removed. Numbers of GFP-positive cells were counted at 48 h postinfection and plotted. The negative control virus MV-αCD38 displays a CD38-specific scFv and does not bind HER2/neu. (B, C, and D) We next determined the impact of receptor affinity on viral infectivity with high-HER2-expressing SKOV3ip.1 cells or low-HER2-expressing TE671 cells (40-fold fewer HER2 receptors). CHO cells expressing the pseudoreceptor αHis were used as a positive control for virus infectivity. Cells were infected at an MOI of 1.0 or 4.0, and the numbers of GFP-positive cells were counted by flow cytometry at 48 h postinfection. Error bars represent standard deviations. *P* value was determined by one-way analysis of variance at an MOI of 4.0. Asterisks (**) indicate a significant difference ($P < 0.01$) between the test group and the MV-αHER-8-infected cells, using Dunnett's multiple comparison test.

positive cells were counted. According to this assay, there was no correlation between the affinities of the viruses for HER2 and their efficiencies of binding to HER2 receptors on SKOV3.ip cells (Fig. 2A). No significant differences in the binding of the viruses to SKOV3ip.1 cells were detected using another assay in which the viruses were allowed to bind to 1% paraformaldehyde-fixed SKOV3ip.1 cells at 37°C, the cells were washed to remove unbound virus and overlaid with Vero-αHis cells, and the numbers of GFP-positive cells were counted (data not shown). To test the impact of receptor affinity on the efficiency and kinetics of MV entry, HER2 receptor-positive human ovarian SKOV3ip.1 cancer cells and CHO-αHis cells were infected with the panel of retargeted viruses at two different MOIs (4.0 and 1.0). A FIP was added at 2 h postinfection to facilitate analysis of the percentage of GFP-positive (virus-infected) cells by flow cytometry. As shown in Fig. 2B, the lower-affinity viruses, strains MV-αHER-6 and -7, were less efficient at using HER2 to gain entry into SKOV3ip.1 cells, while they had similarly high levels of efficiency in infecting CHO-αHis cells (Fig. 2C). An unexpected finding from this study was that the infectious titers of the four higher affinity viruses, strains MV-αHER-8, -9, -10, and -11, did not differ from each other on SKOV3ip.1 cells. Thus, the infectious titer reached its maximum level at a HER2 receptor affinity of 1.6×10^{-8} M and did not increase thereafter, even when the affinity was approximately 1,000-fold increased (to 1.5×10^{-11} M).

TE671 cells expressed lower numbers of HER2 receptors (4.3×10^3/cell) than SKOV3ip.1 cells (1.5×10^5/cell). We therefore tested the infectivity of the HER2-retargeted viruses with TE671 cells at two different MOIs. Similar to the findings with SKOV3ip.1 cells, the viruses with lower affinities showed only background levels of infectivity, whereas the higher affinity viruses were fully infectious (Fig. 2D). Thus, there was, again, a threshold affinity level (1.0×10^{-9} M) below which infectivity was severely compromised and above which infectivity was optimal. There was a trend toward further increases in the infectivity of viruses, with HER2 affinities approximately 10- or 100-fold higher than the threshold required for optimal entry, although these were not significant differences. The most important difference between the TE671 cells and the SKOV3ip.1 cells was that the two cell lines have different affinity thresholds for optimal infectivity of HER2-retargeted viruses. Thus, the affinity of the scFv displayed with the MV-αHER-8 virus is above the threshold for efficient entry into SKOV3ip.1 cells but falls below the threshold required for efficient entry into TE671 cells, which express approximately 40-fold fewer HER2 receptors than the SKOV3ip1 cells. Similar results were observed for another HER2 low-expressing cell line, MDA-MB-231 (data not shown). Thus, the efficiency of viral entry is correlated with the affinity of the attachment protein and the receptor interaction, and there is a loss of infectivity with low-receptor-expressing cells for an otherwise functional affinity.

Receptor affinity and cell-cell fusion. MV entry and cell-to-cell fusion are both mediated by the concerted action of viral attachment (HA) and fusion (F) proteins, but the topologies of the two processes differ, and they might therefore be differen-

TABLE 2. Impact of receptor affinity on virus-induced intercellular fusion[a]

Virus	No. of syncytia ± SD counted in	
	SKOV3ip.1 cells	TE671 cells
MV-aHER-6	9.1 + 6.7*[b]	3.6 + 1.6
MV-aHER-7	10.8 + 6.3*	5.4 + 1.6
MV-aHER-8	91.4 + 22.9	14.1 + 5.6
MV-aHER-9	132.6 + 52.6*	295.2 + 45.9*
MV-aHER-10	152.5 + 32.2*	320.1 + 74.6*
MV-aHER-11	156.2 + 28.3*	327.5 + 36.9*

[a] SKOV3ip.1 cells and TE671 cells were infected with each of the HER2-retargeted measles viruses (MOI of 0.1), and the syncytial indices were determined. Briefly, at 72 h postinfection, cells were fixed and stained with Hoechst 33342. Numbers of nuclei in each syncytium were counted (syncytial index, n = 10 syncytia counted). TE671 cells express 40-fold lower levels of HER2 receptors. Values shown are means ± standard deviations (SD). P value was determined by one-way analysis of variance.

[b] *, indicates a significant difference ($P < 0.01$) between the test group and MV-αHER-8-infected cells, using Dunnett's multiple comparison test.

tially impacted by changes in HA protein receptor affinity. To evaluate the impact of receptor affinity on the kinetics of intercellular fusion, semiconfluent SKOV3ip.1 cell monolayers were infected with each member of the panel of HER2-retargeted viruses and analyzed by microscopy at 72 h after infection. All of the HER2-retargeted viruses efficiently induced extensive cell fusion with Vero-αHis cells via the His_6 tag (data not shown). The extent of virus-induced cell-to-cell fusion was quantitated by measuring the syncytial index (the numbers of nuclei per syncytium). The MV-αHER-8, -9, -10, and -11 efficiently induced extensive intercellular fusion via the HER2 receptor in the SKOV3ip.1 cells, whereas MV-αHER-6 and -7 did not (Table 2). When the SKOV3ip.1 cells were exposed to a high titer of MV-αHER-7, there was an increase in the number of infected (GFP-positive) cells but still no observable syncytial cytopathic effect (Fig. 3). To determine whether cell fusion was simply delayed as opposed to being abrogated in SKOV3ip1 cells infected with the lower affinity viruses, we continued to observe the MV-αHER-7-infected cells until day 6 postinfection. By that late time point there were still no visible syncytia, but each of the infected cells had divided, giving rise to scattered clusters of unfused GFP-positive cells (data not shown). It is apparent from these data that, as in the case of viral entry, there is a threshold level of receptor affinity below which intercellular fusion is absent and above which intercellular fusion proceeds efficiently. Further increases of affinity, up to 1,000-fold above this threshold, did not contribute to further increases in syncytial size.

Oncolytic MV kills cells by inducing intercellular fusion, and the syncytia eventually die by apoptosis (8). We previously documented that the cytopathic potential of oncolytic measles viruses is closely correlated to their ability to cause intercellular fusion (2). The levels of SKOV3ip.1 and TE671 cell viability were therefore estimated by measuring the amount of virus-induced apoptosis and by clonogenicity studies after these cells were infected with each of the HER2-retargeted viruses (Fig. 4). As expected, HER2-dependent cell killing was significant only when viruses with HER2 affinities above the previously determined threshold were used.

In a previous study, we explored the relationship between CD46 receptor density and intercellular fusion in cells infected with an oncolytic MV and showed that fusion proceeded efficiently only above a certain threshold of CD46 receptor density (2). To investigate the relationships among the affinity of viral binding to HER2, the density of HER2 receptors on the target cells, and the efficiency of cell fusion and killing, we assembled a panel of human tumor cell lines and determined the numbers of HER2 receptors on their surfaces by using Becton Dickinson QuantiBrite beads, as described in Materials and Methods. HER2 receptor densities with these cell lines range from undetectable to 3.0×10^5 receptor sites per cell. This panel of cells was infected with each of the six HER2-retargeted viruses at an MOI of 1.0. As shown in Fig. 5, none of the viruses caused intercellular fusion in cells lacking HER2 receptors. However, in HER2-positive cells, there is a clear relationship between the surface density of HER2 receptors and the ability of each of the retargeted viruses to mediate intercellular fusion, depending on its HER2 binding affinity. Thus, MV-αHER-6 and -7 did not induce syncytial formation in any of the

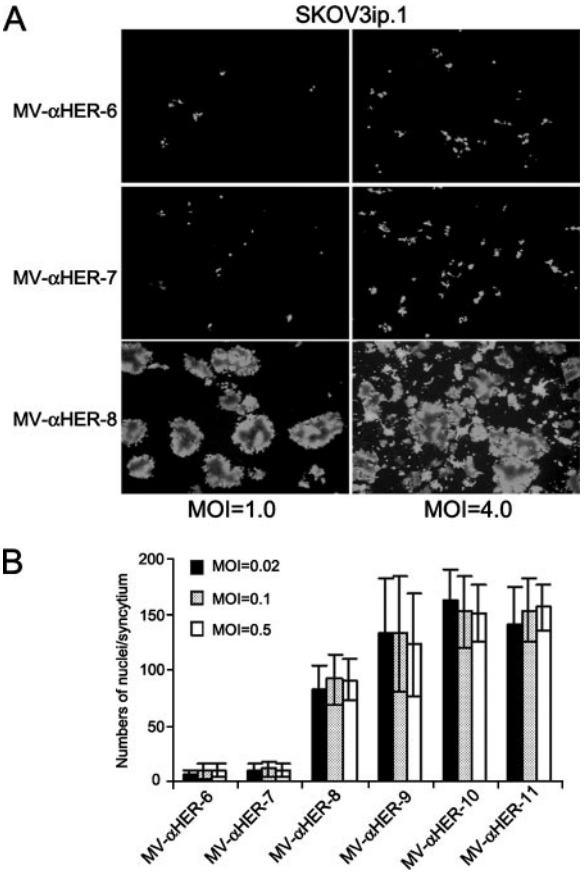

FIG. 3. Influence of MOI on syncytial formation of low- and high-affinity viruses. (A) HER2-overexpressing SKOV3ip.1 cells were infected at MOIs of 1.0 and 4.0 with retargeted viruses. Photographs were taken at 72 h postinfection, and syncytial formations were compared. Increasing the numbers of infectious centers by increasing MOI did not result in syncytial formation for the low-affinity viruses. (B) SKOV3ip.1 cells were infected with each member of the HER2-retargeted virus panel at MOIs of 0.02, 0.1, and 0.5. Cells were fixed and stained with Hoechst 33342 at 72 h postinfection. Numbers of nuclei in each syncytium were counted (10 to 20 syncytia were counted). Sizes of the syncytia were not affected by MOI and were comparable at all MOIs.

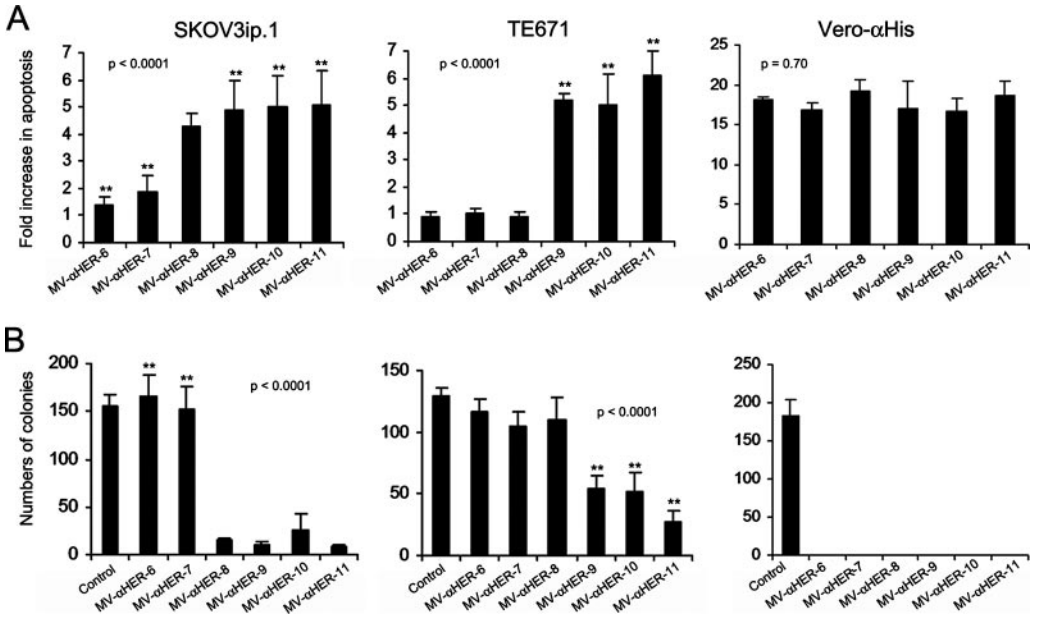

FIG. 4. Cytopathic potential of the HER2-retargeted measles viruses. HER2-overexpressing SKOV3ip.1 cells, low-HER2-expressing TE671 cells, and Vero-αHis cells were infected with HER2-retargeted viruses at an MOI of 1.0. Virus-induced apoptosis (A) and antiproliferative effects (B) were analyzed by enzyme-linked immunosorbent assay and by clonogenic assay, respectively. Error bars represent ± standard deviations. The *P* value was determined by one-way analysis of variance. Asterisks (**) indicate a significant difference ($P < 0.01$) between the test group and the MV-αHER-8-infected group, using Dunnett's multiple comparison test.

HER2-positive cell lines tested, except in the AU-565 cells with the highest expression of HER2. MV-αHER-8, which caused extensive intercellular fusion in SKOV3ip.1 cells, did not induce cell fusion in tumor cells expressing low to intermediate levels of HER2 receptors. The MV-αHER-9, -10, and -11 displaying higher-affinity scFvs induced large syncytia, even in cells expressing only 3,000 HER2 receptor sites. It is evident from these data that the affinity level of HER2 binding needed to trigger lethal intercellular fusion is inversely correlated to the HER2 receptor density; that is to say, a higher scFv receptor affinity is required to mediate the fusion and killing of tumor cells with lower HER2 receptor numbers.

To confirm that these data were not unduly influenced by the use of different types of human cell lines, we transfected a HER2 expression plasmid to generate CHO cell clones expressing different surface levels of HER2 receptors. We selected CHO-HER2 no. 1 (3.1×10^3 HER2/cell) and CHO-HER2 no. 6 (8.0×10^4 HER2/cell) as the low- and high-HER2-expressing cells, respectively. As shown in Fig. 5, the syncytial affinity threshold was readily apparent with these cells, and the threshold was higher at lower receptor densities. Interestingly, MV-αHER-9 was able to infect the CHO clone expressing the lower density of HER2 receptors, but intercellular fusion was not observed after infection with this virus. A syncytial cytopathic effect was readily apparent when these cells were infected with the two highest-affinity virus strains, MV-αHER-10 and -11. These data confirm that the threshold HER2 receptor affinity level required for intercellular fusion and tumor cell killing varies inversely with the density of HER2 receptors present on the target cell surface.

DISCUSSION

Oncolytic attenuated Edmonston strain measles viruses are being developed as anticancer therapeutics. To improve virus accuracy and to minimize toxicity, MV interaction with its two cognate receptors, the ubiquitously expressed CD46 and SLAM, which is associated with measles-induced immunosuppression (16, 27), can be fully ablated. Viral infection and cytopathic killing can be redirected exclusively to cancer cells by the display of scFvs on the C terminus of the ablated HA protein to mediate highly efficient viral entry and cytopathic effects via CD38, EGFR, EGFRvIII, and the alpha-folate receptor (11, 12, 22). The interaction of the viral attachment protein with the targeted receptor plays a critical role in determining the specificity and performance of the retargeted virus. As such, variables that influence the interaction between the viral attachment protein and its receptor, such as receptor affinity (k_{on} and k_{off}) or accessibility and abundance of the receptor, should be considered in the vector design. Indeed, the receptor affinity, the receptor density, and the binding avidity of the viral particle are interrelated. Research using tumor-targeted scFvs clearly indicate that increasing the numbers of binding domains that interact with the receptor (increased valency) can compensate for low-affinity binders (1). Indeed, dimerization of a low-affinity scFv is a more attractive and less tedious method with which to obtain agents with greater tumor targeting and localization than exhaustive scFv affinity maturation (26). As such, it is often argued that high avidity due to multivalent viral attachment protein binding with "sufficient" numbers of cognate receptors should compensate for low-affinity receptor binding interactions and lead to

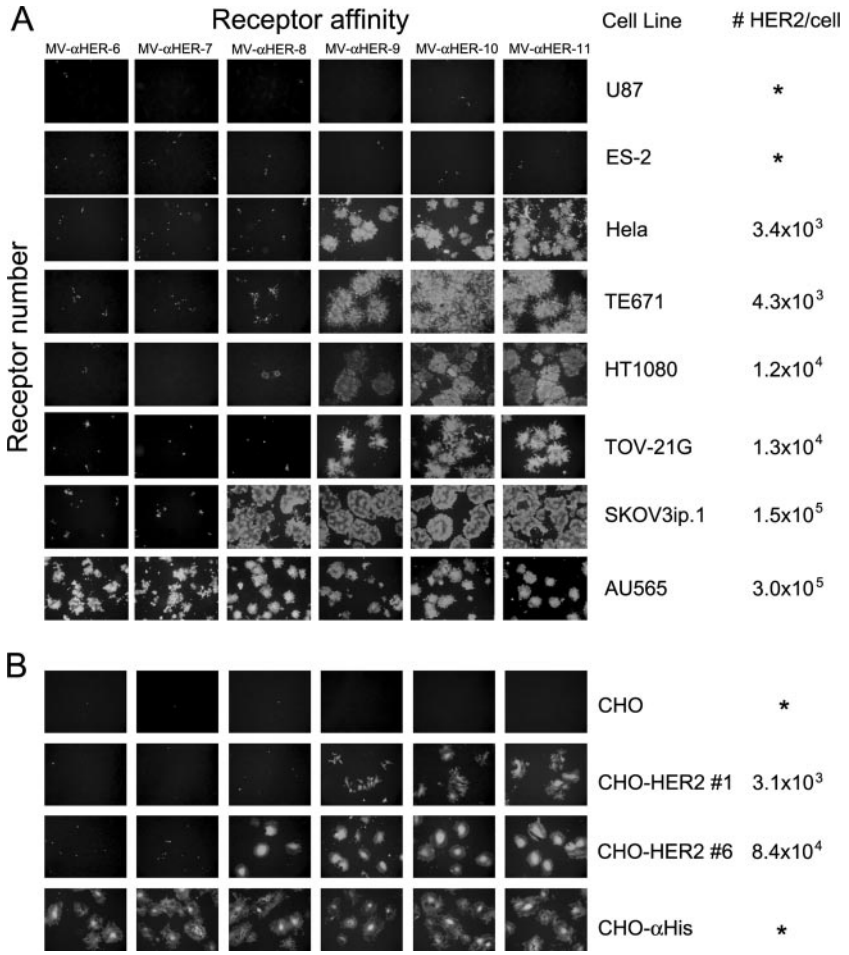

FIG. 5. The impact of HER2 receptor density and affinity with virus-induced cell-to-cell fusion. (A) A panel of tumor cell lines with various amounts of HER2 receptors was infected with each of the HER2-retargeted viruses at an MOI of 1.0. Asterisks (*) denote receptor levels below the levels of detection (10^3). Photographs were taken at 72 h postinfection. (B) CHO cells or CHO clones expressing low and high HER2 receptors and CHO-αHis cells were treated as shown in panel A.

efficient viral attachment and entry (17). However, data presented here clearly demonstrate that the relationship is not that straightforward and, importantly, a threshold receptor affinity is required to mediate optimal viral entry and virus-induced intercellular fusion.

Paramyxovirus attachment and fusion functions are performed by two separate proteins (9). The HA attachment protein is a type II glycoprotein and is a tetramer composed of two homodimers, while F is a type I glycoprotein and a trimer (15). The HA and F proteins each have short cytoplasmic tails embedded in the matrix protein just underlying the envelope coat membrane of the virion. The HA and F proteins are thought to be closely associated, probably by noncovalent interactions (9). The spatial orientation of each HA tetramer relative to that of F is unknown, but a model in which the parainfluenza virus HA tetramers are tilted at a 45° angle, with the trimeric F protein aligned between, has been proposed (51). Results from the virus binding assay did not show a correlation between the receptor affinity and the kinetics of viral attachment to HER-2-positive SKOV3ip.1 cells. This observation is not unexpected and is likely due to the multivalent nature of viral attachment and the very-high-associated viral binding avidity. The six HER2 scFvs have comparable k_{on} values but very different k_{off} values (38). However, once the virus gets near the surface of the cell by random chance and binds to the cell, it is unlikely to detach from it because of the hundreds of copies of the HA attachment protein on the virion's surface that can interact with nearby receptors. In contrast to viral binding, there was a clear dependence on receptor affinity in mediating viral entry and infection. One model, consistent with our data, proposes that HA proteins trigger F protein activation only if they have been in complex with their receptors for a finite period and that membrane fusion proceeds only if F protein activation reaches a critical intensity at the site of membrane contact. At higher affinities, associated with slower k_{off} rates, a given HA protein-receptor interaction has greater longevity and is therefore more likely to trigger a conformational rearrangement of the F protein. The number of HA-receptor interactions that last long enough to trigger conformational F protein rearrangements (i.e., the fusion threshold) is therefore predicted to be a function of three factors: the density of HA proteins on the donor membrane, the density of receptor sites on the target

membrane, and the k_{off} rates of the HA-receptor complexes. These predictions are supported by our data. The binding affinities of the displayed antibodies correlate closely to their k_{off} values, which range from 130×10^{-3} s^{-1} ($K_d = 1.6 \times 10^{-6}$ M) to 0.015×10^{-3} s^{-1} ($K_d = 1.5 \times 10^{-11}$ M) (37, 38).

The binding affinities of measles HA protein for CD46 and SLAM have been measured, and the dissociation constant values are in the range of 1×10^{-7} M for CD46 and 5×10^{-7} M for SLAM (36). In this regard, it is interesting to note that for efficient cell fusion, the k_{off} values are in a similar range for the CD46 (7.4×10^{-3} s^{-1}) and the anti-HER2 C6.5 (6.3×10^{-3} s^{-1}) scFvs. However, it is apparent that the highly efficient usage of CD46 for viral infection and for intercellular fusion is able to occur at an affinity rate that is significantly lower than for some viruses, such as HIV binding to CD4 (K_d, $\sim 10^{-9}$ M) (49).

Closer analysis of the data shown in Fig. 2 and 3 reveals that there are subtle differences in the affinity thresholds for viral entry and intercellular fusion. For many of the cells that were tested, the threshold affinity for viral entry appears to be slightly lower than the threshold affinity for intercellular fusion. This is particularly apparent in a comparison of the photographs of CHO-HER2 no. 1 cells infected with MV-αHER-9 and those showing CHO-HER2 cells infected with MV-αHER-10 (Fig. 5). Entry is efficient, but intercellular fusion is impaired in the MV-αHER-9-infected cells, whereas intercellular fusion proceeds with high efficiency after infection with MV-αHER-10. A possible explanation for this small but definite difference in the affinity thresholds for cell entry and intercellular fusion may be that the density of HA proteins is higher on the viral particles (virus-cell fusion) than it is on the infected cells (cell-cell fusion).

In conclusion, we have generated a panel of six HER2-specific recombinant measles viruses displaying affinity-mutated scFvs that bind to a single epitope on the HER2/neu receptor with a 5-log difference in affinity, and we used these viruses to explore the relationship between receptor affinity and receptor density in viral entry, intercellular fusion, or cytopathic potency in HER2-positive tumor cells. This is the first comprehensive analysis of the impact of receptor affinity with virus-cell interactions. The results are quite unexpected, showing that there is a functional threshold affinity level above which infection and intercellular fusion proceed with equal efficiency, even over a 1,000-fold affinity range; below the threshold, infection is minimal. The threshold correlates inversely with receptor density such that higher affinities are required to infect cells with lower receptor densities. Thus, depending on their receptor affinities, enveloped viruses can discriminate between cells expressing different densities of a targeted receptor.

ACKNOWLEDGMENTS

This work was supported by funds from the National Institutes of Health (grant CA118488 to K.-W.P. and grant CA100634 to S.J.R.) and the Mayo Clinic Cancer Center.

REFERENCES

1. **Adams, G. P., M. S. Tai, J. E. McCartney, J. D. Marks, W. F. Stafford III, L. L. Houston, J. S. Huston, and L. M. Weiner.** 2006. Avidity-mediated enhancement of in vivo tumor targeting by single-chain Fv dimers. Clin. Cancer Res. **12:**1599–1605.
2. **Anderson, B. D., T. Nakamura, S. J. Russell, and K. W. Peng.** 2004. High CD46 receptor density determines preferential killing of tumor cells by oncolytic measles virus. Cancer Res. **64:**4919–4926.
3. **Bookman, M. A., K. M. Darcy, D. Clarke-Pearson, R. A. Boothby, and I. R. Horowitz.** 2003. Evaluation of monoclonal humanized anti-HER2 antibody, trastuzumab, in patients with recurrent or refractory ovarian or primary peritoneal carcinoma with overexpression of HER2: a phase II trial of the Gynecologic Oncology Group. J. Clin. Oncol. **21:**283–290.
4. **Dingli, D., K. W. Peng, M. E. Harvey, P. R. Greipp, M. K. O'Connor, R. Cattaneo, J. C. Morris, and S. J. Russell.** 2004. Image-guided radiovirotherapy for multiple myeloma using a recombinant measles virus expressing the thyroidal sodium iodide symporter. Blood **103:**1641–1646.
5. **Dorig, R. E., A. Marcil, A. Chopra, and C. D. Richardson.** 1993. The human CD46 molecule is a receptor for measles virus (Edmonston strain). Cell **75:**295–305.
6. **Enders, J. F., and T. C. Peebles.** 1954. Propagation in tissue cultures of cytopathogenic agents from patients with measles. Proc. Soc. Exp. Biol Med. **86:**277–286.
7. **Enders, J. F., T. C. Peebles, K. McCarthy, M. Milovanovic, A. Mitus, and A. Holloway.** 1957. Measles virus: a summary of experiments concerned with isolation, properties, and behavior. Am. J. Public Health **47:**275–282.
8. **Galanis, E., A. Bateman, K. Johnson, R. M. Diaz, C. D. James, R. Vile, and S. J. Russell.** 2001. Use of viral fusogenic membrane glycoproteins as novel therapeutic transgenes in gliomas. Hum. Gene Ther. **12:**811–821.
9. **Griffin, D.** 2001. Measles virus, p. 1401. *In* D. Knipe, P. Howley, D. Griffin, R. Lamb, M. Martin, B. Roizman, and S. Straus (ed.), Fields virology 4th ed., vol. 1. Lippincott Williams & Wilkins, Philadelphia, PA.
10. **Grote, D., S. J. Russell, T. I. Cornu, R. Cattaneo, R. Vile, G. A. Poland, and A. K. Fielding.** 2001. Live attenuated measles virus induces regression of human lymphoma xenografts in immunodeficient mice. Blood **97:**3746–3754.
11. **Hadac, E. M., K. W. Peng, T. Nakamura, and S. J. Russell.** 2004. Reengineering paramyxovirus tropism. Virology **329:**217–225.
12. **Hasegawa, K., T. Nakamura, M. Harvey, Y. Ikeda, A. Oberg, M. Figini, S. Canevari, L. C. Hartmann, and K. W. Peng.** 2006. The use of a tropism-modified measles virus in folate receptor-targeted virotherapy of ovarian cancer. Clin. Cancer Res. **12:**6170–6178.
13. **Hasegawa, K., L. Pham, M. K. O'Connor, M. J. Federspiel, S. J. Russell, and K. W. Peng.** 2006. Dual therapy of ovarian cancer using measles viruses expressing carcinoembryonic antigen and sodium iodide symporter. Clin. Cancer Res. **12:**1868–1875.
14. **Hsu, E. C., C. Iorio, F. Sarangi, A. A. Khine, and C. D. Richardson.** 2001. CDw150(SLAM) is a receptor for a lymphotropic strain of measles virus and may account for the immunosuppressive properties of this virus. Virology **279:**9–21.
15. **Lamb, R. A., R. G. Paterson, and T. S. Jardetzky.** 2006. Paramyxovirus membrane fusion: lessons from the F and HN atomic structures. Virology **344:**30–37.
16. **Liszewski, M. K., C. Kemper, J. D. Price, and J. P. Atkinson.** 2005. Emerging roles and new functions of CD46. Springer Semin. Immunopathol. **27:**345–358.
17. **Marsh, M., and A. Helenius.** 2006. Virus entry: open sesame. Cell **124:**729–740.
18. **McDermott, B. M., Jr., A. H. Rux, R. J. Eisenberg, G. H. Cohen, and V. R. Racaniello.** 2000. Two distinct binding affinities of poliovirus for its cellular receptor. J. Biol. Chem. **275:**23089–23096.
19. **Meden, H., and W. Kuhn.** 1997. Overexpression of the oncogene c-erbB-2 (HER2/neu) in ovarian cancer: a new prognostic factor. Eur. J. Obstet Gynecol. Reprod. Biol. **71:**173–179.
20. **Meric-Bernstam, F., and M. C. Hung.** 2006. Advances in targeting human epidermal growth factor receptor-2 signaling for cancer therapy. Clin. Cancer Res. **12:**6326–6330.
21. **Mizuguchi, H., and T. Hayakawa.** 2004. Targeted adenovirus vectors. Hum. Gene. Ther. **15:**1034–1044.
22. **Nakamura, T., K. W. Peng, M. Harvey, S. Greiner, I. A. Lorimer, C. D. James, and S. J. Russell.** 2005. Rescue and propagation of fully retargeted oncolytic measles viruses. Nat. Biotechnol. **23:**209–214.
23. **Nakamura, T., K. W. Peng, S. Vongpunsawad, M. Harvey, H. Mizuguchi, T. Hayakawa, R. Cattaneo, and S. J. Russell.** 2004. Antibody-targeted cell fusion. Nat. Biotechnol. **22:**331–336.
24. **Naniche, D., G. Varior-Krishnan, F. Cervoni, T. F. Wild, B. Rossi, C. Rabourdin-Combe, and D. Gerlier.** 1993. Human membrane cofactor protein (CD46) acts as a cellular receptor for measles virus. J. Virol. **67:**6025–6032.
25. **Natali, P. G., M. R. Nicotra, A. Bigotti, I. Venturo, D. J. Slamon, B. M. Fendly, and A. Ullrich.** 1990. Expression of the p185 encoded by HER2 oncogene in normal and transformed human tissues. Int. J. Cancer **45:**457–461.
26. **Nielsen, U. B., G. P. Adams, L. M. Weiner, and J. D. Marks.** 2000. Targeting of bivalent anti-ErbB2 diabody antibody fragments to tumor cells is independent of the intrinsic antibody affinity. Cancer Res. **60:**6434–6440.
27. **Ohno, S., N. Ono, F. Seki, M. Takeda, S. Kura, T. Tsuzuki, and Y. Yanagi.**

2007. Measles virus infection of SLAM (CD150) knockin mice reproduces tropism and immunosuppression in human infection. J. Virol. **81:**1650–1659.
28. **Ong, H. T., M. M. Timm, P. R. Greipp, T. E. Witzig, A. Dispenzieri, S. J. Russell, and K. W. Peng.** 2006. Oncolytic measles virus targets high CD46 expression on multiple myeloma cells. Exp. Hematol. **34:**713–720.
29. **Pegram, M., and D. Slamon.** 2000. Biological rationale for HER2/neu (c-erbB2) as a target for monoclonal antibody therapy. Semin. Oncol. **27:**13–19.
30. **Peng, K. W., G. J. Ahmann, L. Pham, P. R. Greipp, R. Cattaneo, and S. J. Russell.** 2001. Systemic therapy of myeloma xenografts by an attenuated measles virus. Blood **98:**2002–2007.
31. **Peng, K. W., and S. J. Russell.** 1999. Viral vector targeting. Curr. Opin. Biotechnol. **10:**454–457.
32. **Peng, K. W., C. J. TenEyck, E. Galanis, K. R. Kalli, L. C. Hartmann, and S. J. Russell.** 2002. Intraperitoneal therapy of ovarian cancer using an engineered measles virus. Cancer Res. **62:**4656–4662.
33. **Phuong, L. K., C. Allen, K. W. Peng, C. Giannini, S. Greiner, C. J. TenEyck, P. K. Mishra, S. I. Macura, S. J. Russell, and E. C. Galanis.** 2003. Use of a vaccine strain of measles virus genetically engineered to produce carcinoembryonic antigen as a novel therapeutic agent against glioblastoma multiforme. Cancer Res. **63:**2462–2469.
34. **Press, M. F., C. Cordon-Cardo, and D. J. Slamon.** 1990. Expression of the HER-2/neu proto-oncogene in normal human adult and fetal tissues. Oncogene **5:**953–962.
35. **Roskoski, R., Jr.** 2004. The ErbB/HER receptor protein-tyrosine kinases and cancer. Biochem. Biophys. Res. Commun. **319:**1–11.
36. **Santiago, C., E. Bjorling, T. Stehle, and J. M. Casasnovas.** 2002. Distinct kinetics for binding of the CD46 and SLAM receptors to overlapping sites in the measles virus hemagglutinin protein. J. Biol. Chem. **277:**32294–32301.
37. **Schier, R., J. D. Marks, E. J. Wolf, G. Apell, C. Wong, J. E. McCartney, M. A. Bookman, J. S. Huston, L. L. Houston, L. M. Weiner, et al.** 1995. In vitro and in vivo characterization of a human anti-c-erbB-2 single-chain Fv isolated from a filamentous phage antibody library. Immunotechnology **1:**73–81.
38. **Schier, R., A. McCall, G. P. Adams, K. W. Marshall, H. Merritt, M. Yim, R. S. Crawford, L. M. Weiner, C. Marks, and J. D. Marks.** 1996. Isolation of picomolar affinity anti-c-erbB-2 single-chain Fv by molecular evolution of the complementarity determining regions in the center of the antibody binding site. J. Mol. Biol. **263:**551–567.
39. **Serrano-Olvera, A., A. Duenas-Gonzalez, D. Gallardo-Rincon, M. Candelaria, and J. De la Garza-Salazar.** 2006. Prognostic, predictive and therapeutic implications of HER2 in invasive epithelial ovarian cancer. Cancer Treat. Rev. **32:**180–190.
40. **Skehel, J. J., and D. C. Wiley.** 2000. Receptor binding and membrane fusion in virus entry: the influenza hemagglutinin. Annu. Rev. Biochem. **69:**531–569.
41. **Slamon, D. J., G. M. Clark, S. G. Wong, W. J. Levin, A. Ullrich, and W. L. McGuire.** 1987. Human breast cancer: correlation of relapse and survival with amplification of the HER-2/neu oncogene. Science **235:**177–182.
42. **Slamon, D. J., B. Leyland-Jones, S. Shak, H. Fuchs, V. Paton, A. Bajamonde, T. Fleming, W. Eiermann, J. Wolter, M. Pegram, J. Baselga, and L. Norton.** 2001. Use of chemotherapy plus a monoclonal antibody against HER2 for metastatic breast cancer that overexpresses HER2. N. Engl. J. Med. **344:**783–792.
43. **Snyder, G. A., J. Ford, P. Torabi-Parizi, J. A. Arthos, P. Schuck, M. Colonna, and P. D. Sun.** 2005. Characterization of DC-SIGN/R interaction with human immunodeficiency virus type 1 gp120 and ICAM molecules favors the receptor's role as an antigen-capturing rather than an adhesion receptor. J. Virol. **79:**4589–4598.
44. **Stuart, D. I., and E. Y. Jones.** 1995. Recognition at the cell surface: recent structural insights. Curr. Opin. Struct. Biol. **5:**735–743.
45. **Takemoto, D. K., J. J. Skehel, and D. C. Wiley.** 1996. A surface plasmon resonance assay for the binding of influenza virus hemagglutinin to its sialic acid receptor. Virology **217:**452–458.
46. **Tatsuo, H., N. Ono, K. Tanaka, and Y. Yanagi.** 2000. SLAM (CDw150) is a cellular receptor for measles virus. Nature **406:**893–897.
47. **Ugolini, S., I. Mondor, and Q. J. Sattentau.** 1999. HIV-1 attachment: another look. Trends Microbiol. **7:**144–149.
48. **Vongpunsawad, S., N. Oezgun, W. Braun, and R. Cattaneo.** 2004. Selectively receptor-blind measles viruses: identification of residues necessary for SLAM- or CD46-induced fusion and their localization on a new hemagglutinin structural model. J. Virol. **78:**302–313.
49. **Wang, J.** 2002. Protein recognition by cell surface receptors: physiological receptors versus virus interactions. Trends Biochem. Sci. **27:**122–126.
50. **Wickham, T. J.** 2003. Ligand-directed targeting of genes to the site of disease. Nat. Med. **9:**135–139.
51. **Yuan, P., T. B. Thompson, B. A. Wurzburg, R. G. Paterson, R. A. Lamb, and T. S. Jardetzky.** 2005. Structural studies of the parainfluenza virus 5 hemagglutinin-neuraminidase tetramer in complex with its receptor, sialyllactose. Structure **13:**803–815.